Journal of Colloid and Interface Science 336 (2009) 171–175

Contents lists available at ScienceDirect

Journal of Colloid and Interface Science

www.elsevier.com/locate/jcis

Hexanedioic acid mediated surface–ligand-exchange process for transferring $NaYF_4$:Yb/Er (or Yb/Tm) up-converting nanoparticles from hydrophobic to hydrophilic

Qingbin Zhang [a,b], Kai Song [a,b], Junwei Zhao [a,b], Xianggui Kong [a,*], Yajuan Sun [a], Xiaomin Liu [a], Youlin Zhang [a], Qinghui Zeng [a], Hong Zhang [c,*]

[a] Key Laboratory of Excited State Process, Changchun Institute of Optics, Fine Mechanics and Physics, Chinese Academy of Sciences, Changchun 130033, PR China
[b] Graduate School of Chinese Academy of Sciences, Beijing 100039, PR China
[c] Van't Hoff Institute for Molecular Sciences, University of Amsterdam, Nieuwe Achtergracht 166, 1018 WV Amsterdam, The Netherlands

ARTICLE INFO

Article history:
Received 23 January 2009
Accepted 1 April 2009
Available online 14 April 2009

Keywords:
Nanoparticles
Upconversion
$NaYF_4$
Hexanedioic acid
Ligand exchange
Biological application

ABSTRACT

Water-soluble and carboxyl-functionalized up-converting rare-earth nanoparticles (UCNPs) are obtained via an efficient surface–ligand-exchange procedure. Hexanedioic acid molecules are employed to replace the original hydrophobic ligands in diethylene glycol solvent at high temperature. Various characterizations indicate the ligand-exchange process has negligible adverse effect on the quality of the UCNPs. The resulting hydrophilic UCNPs show small size, strong up-converting emission and high water stability. The specific molecular recognition capacity of avidin-modified hydrophilic UCNPs confirms that hydrophilic UCNPs are suitable for potential biological labeling.

1. Introduction

In the past few years, up-converting rare-earth nanoparticles (UCNPs) have shown great potential as a new class of fluorophores for biological and biomedical applications [1–3]. In comparison with conventional downconversion fluorescent materials, including organic dyes [4] and semiconductor quantum dots (QDs) such as CdS, CdSe and CdTe, etc. [5–7], the UCNPs have many advantages, such as high penetration depth and low background fluorescence due to excitation in near infrared and nearly absence of photo-damage under low power excitation [2,8–10].

Generally, synthesis of high-quality UCNPs is performed in organic solvents with surface passivation by long hydrocarbon chains of the surfactants. This nonaqueous method is capable of producing colloidal nanocrystals (NCs) with high crystalline, strong upconversion luminescence and narrow particle size distribution, comparing with the synthesis in aqueous solution [11–15]. However, insolubility of the NCs in water greatly limits their biological applications. Yet several strategies have been developed to transfer hydrophobic NCs into hydrophilic (such as Fe_2O_3, rare-earth NCs and QDs, etc.) [16–20]. Among which one is based on the encapsulation of hydrophobic NCs with amphiphilic polymer [21,22] or SiO_2 [23–26]. However, the additional layers of amphiphilic polymer or SiO_2 will dramatically increase the size of the particles which is not desirable for the biological applications, especially for fluorescence resonance energy transfer and in vivo applications [27,28]. Confronted with these challenges, Li et al. recently reported the directly oxidizing oleic acid ligand strategy to transfer UCNPs from hydrophobic to hydrophilic [20]. There are some limitation of this method, such as a relatively long reaction time and low yields, which remain to be solved.

Surface–ligand exchange is an alternative method, which is widely used in QDs. The mainly advantages of the method are simply and the process will not increase the size of the nanoparticles due to the small size of the exchange agents such as mercaptoacetic acid, dihydrolipoic acid and cysteines [28–30]. However, this method relies on the exchange of the surfactant coating ligands with the substitutional molecule of which one end carrying a functional group that is reactive toward the nanocrystal surface and the other end carrying a hydrophilic group. Therefore, it is difficult to have a universal substitutional molecule for all kinds of nanoparticles in ligand-exchange strategy. For this reason, up to date, although the water-soluble UCNPs have been obtained via the methods of oxidizing ligands or encapsulation, no feasible surface–ligand-exchange approach has been developed, owing to the difficulties in obtaining compatible and small substitutional ligands [20]. It is thus desirable to find proper substitutional ligand molecules and to develop a feasible surface–ligand-exchange method for getting the biocompatible water-soluble UCNPs.

* Corresponding authors.
E-mail addresses: xgkong14@ciomp.ac.cn (X. Kong), h.zhang@uva.nl (H. Zhang).

0021-9797/$ - see front matter
doi:10.1016/j.jcis.2009.04.024

In this paper, the hexanedioic acid (HDA) molecules are selected as substitutional ligand, based on the following two reasons. First, the HDA molecule has two —COOH groups which make it in principle possible to coordinate one —COOH group to the UCNPs surface due to strong coordination of —COOH group with lanthanide ions (Ln^{3+}), and to leave the other end —COOH group free for water compatibility. Second, the HDA molecule, owing medial six carbons, proper in length since too short-chain alkanedioic acid will chelate easily to the surface of nanoparticles whereas too long-chain alkanedioic acid will be less favorable in dissolving in water. The ligand-exchange process is performed at relatively high temperature (~240 °C, which is close to DEG solvent boiling point ~245 °C) to enhance the efficiency of the ligand-exchange reaction. Besides, in the reaction system, high concentration (~0.4 mmol/mL) of the HDA molecules is kept to reduce the possibility of chelating of the HDA on the particle surface. The results show that the UCNPs are successfully transferred from hydrophobic to hydrophilic. It is anticipated that this method might be applied to the ligand exchange for other kinds of nanoparticles, which have strong ability of coordination with —COOH group, such as Fe_3O_4, TiO_2 and Au, etc. [31–33]. Scheme 1 schematically illustrates the general principle of the ligand-exchange approach.

The efficient ligand-exchange process is affirmed by various characterizations. The resulting HDA coated UCNPs maintain strong upconversion emission, small size and long term stability in aqueous solution. Moreover, the specific molecular recognition capacity of avidin-modified hydrophilic UCNPs is studied with fluorescence microscopy, indicating that the HDA modified UCNPs are suitable for biological labeling.

2. Materials and methods

2.1. Materials

All the rare-earth trifluoroacetates were prepared by dissolving the respective rare-earth oxides in trifluoroacetic acid (CF_3COOH; 99%, Aldrich). Trifluoroacetic acid sodium salt (CF_3COONa; 97%, Acros), oleylamine (OM; >80%, Acros), hexanedioic acid (HDA, 99%, Tianjin Chemical Co.), diethylene glycol (DEG; 98%, Tianjin Chemical Co.) ethyl-3-dimethyl amino propyl carbodiimide (EDAC, 98%, Aldrich), N-hydroxysulfosuccinimide sodium salt (Sulfo-NHS, Aldrich), bovine serum albumin (BSA), 2-(N-morpholino)ethanesulfonic acid (MES) hydrate, phosphate buffered saline (PBS) buffer, Tween 20, human IgG and bioinylated goat anti-human IgG were purchased from Beijing Dingguo Biotechnology Corporation. All chemical materials were used without further purification.

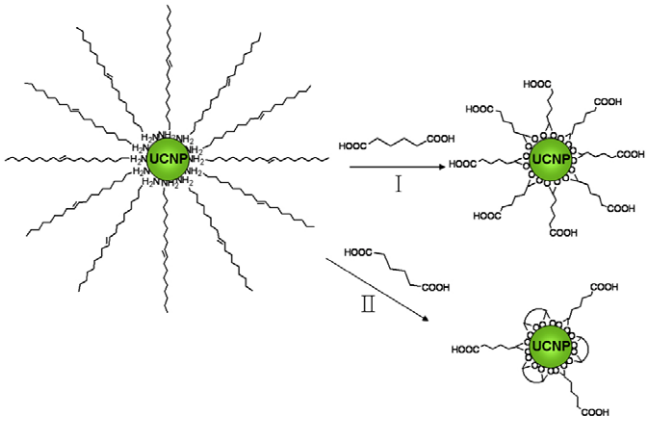

Scheme 1. Schematic illustration of the general principle of ligand-exchange approach using hexanedioic acid as substitutional ligand. I is the ideal model, II is close to actual situation.

2.2. Synthesis of $NaYF_4$:20%Yb, 2% Er (or Tm) NCs

OM coated $NaYF_4$:20% Yb, 2% Er (or Tm, Ho) nanoparticles were synthesized following the routes described previously [12]. Briefly, the mixture of CF_3COONa (2 mmol), $(CF_3COO)_3Y$ (0.78 mmol), $(CF_3COO)_3Yb$ (0.2 mmol), and $(CF_3COO)_3Er$ (or Tm) (0.02 mmol) was dissolved in oleylamine (10 mL), the mixture was then heated to 120 °C to remove water and oxygen, with vigorous magnetic stirring under argon flow for 1 h, followed by 2 h heating at 330 °C in the presence of argon protection. The resulting transparent yellowish reaction mixture was cooled down to 80 °C before ethanol (20 mL) was added. After purification using the standard precipitation–dissolution procedure, the as-synthesized nanoparticles were dissolved in chloroform before further treatment.

2.3. Surface–ligand exchange of UCNPs by HDA

The DEG solution (8.0 mL) containing HDA (500 mg, 3.4 mmol) was heated up to 110 °C with vigorous stirring under argon flow. A chloroform solution of UCNPs (~20 mg) was injected into the hot solution which became turbid immediately. The system was heated to 240 °C and kept at this temperature for about 1.5 h until the solution became clear. After the solution was cooled to room temperature, excess aqueous solution was added, and the NCs were isolated by centrifugation and decantation. Finally the sample was washed three times with pure water and redispersed in deionized water for analysis.

2.4. Bioconjugation of nanoparticles and fluorescence microscope imaging

The experimental processes are as follows: 2.0 mg nanoparticles were suspended in 1.0 mL of 0.02 M MES buffer (pH 6.0), containing 5 mg EDAC and 15 mg sulfo-NHS, and then stirred for 4 h at room temperature. After centrifugation resulting particles were redispersed in MES buffer, and 1 mg avidin was added. The mixture was stirred for 48 h at 4 °C. Finally, the avidin-coated nanoparticles were centrifuged, washed and suspended into 5 mM borate buffer (PH 8.5), containing 1% BSA, 0.05% Tween 20.

Human IgG with concentration of 0.1 mg/mL was spotted manually on an aldehyde silicon surface, allowed to incubate for 2 h at 37 °C. After washing with PBST (PBS containing 0.05% Tween 20) buffer three times, 2% BSA solution was added to block the active sites on the slice for 1 h. Then the silicon slice was put into biotinylated goat anti-human IgG or goat anti-human IgG with concentration of 0.1 mg/mL solution and incubated at 37 °C for 2 h. After washed with PBST and deionized water, the silicon wafers subjected to fluorescent microscopy. Slices were examined under a Motic AE30 microscope equipped with a Canon A630 camera. The excited light comes from an adscititious semiconductor diode laser with 980 nm.

2.5. Characterization

Morphology of the UCNPs was characterized at 200 kV using a Hitachi H-8100 IV transmission electron microscopy (TEM). The mean hydrodynamic size and size distribution were determined by dynamic light scattering (DLS) using Zetasizer 3000HSA. The ligand exchange was identified by Fourier transform infrared spectra (FT-IR, Perkin-Elmer spectrophotometer) and thermogravimetric analysis (TGA, Perkin-Elmer TGA-7). The upconversion emission spectra were recorded by a Jobin-Yvon LabRam Raman spectrometer system equipped with a Peltier air-cooled CCD detector excited by 980 nm laser. The fluorescence microscope imaging was taken under a Motic AE30 microscope equipped with a Canon A630 camera excited by a semiconductor diode laser

with 980 nm. X-ray diffraction (XRD) measurements were performed with a Rigaku D/max-2000 diffractometer using CuKα radiation (λ = 1.5406 Å).

3. Results and discussion

3.1. Morphology and hydrodynamic size of the nanocrystals

Fig. 1 gives TEM images of original and HDA capped $NaYF_4$:20% Yb, 2% Er UCNPs. As is shown in Fig. 1(a), the original UCNPs are spherical and nearly monodispersed, with an average diameter of about 12 nm. Compared with the original UCNPs, the size and shape of the HDA capped UCNPs (Fig. 1(b)) have no obvious changes. Similar TEM results are also observed for $NaYF_4$:20% Yb, 2% Tm UCNPs (see Fig. S1 of the Supporting Information).

HDA is a small water-soluble molecule with two carboxyl groups and can form a thin hydrophilic surfactant layer on UCNPs surface. To estimate the hydrodynamic diameter of the particles in solution, dynamic light scattering (DLS) was employed. The hydrophilic UCNPs exhibit narrow hydrodynamic size distribution with the mean hydrodynamic diameters of 13.0 nm (Fig. 2). The small hydrodynamic size is desirable for biological applications.

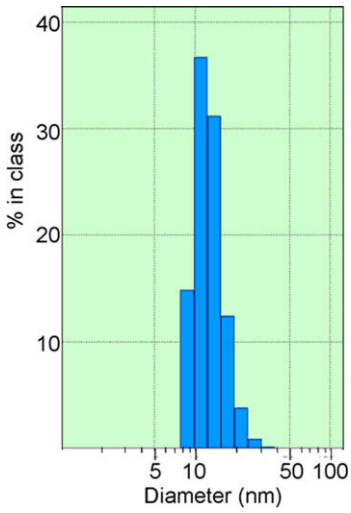

Fig. 2. Hydrodynamic diameter distribution of the HDA coated $NaYF_4$:Yb/Er UCNPs in water, as determined by dynamic light scattering.

3.2. Analysis of surface–ligand-exchange process

It is necessary to point that a few factors i.e. high temperature, excess robust adhesion ligand and appropriate solvent affect the successful ligand-exchange reaction. In our case, the ligand-exchange reaction was performed at high temperature (~240 °C), which is close to DEG solvent boiling point (~245 °C), with the consideration that dynamic solvation of the ligands favors the exchange of original surfactants with new ones [19]. Besides, in the reaction system large excess HDA molecules exist (3.4 mmol) which is positive for the ligand-exchange reaction. Moreover, the HDA ligand has more anchoring points than OM ligand and the coordinating ability of —COO^- group from HDA with rare-earth ions is also stronger than that of —NH_2 from OM. Thus, high exchange efficiency is expected. The obtained hydrophilic UCNPs can be stably dispersed in water for one month, without obvious sedimentation.

FT-IR spectra of the UCNPs before and after ligand exchange are shown in Fig. 3(a). In Fig. 3(a)-A, 1084 cm^{-1} and 1581 cm^{-1} are assigned to C—N stretch and —NH2 deformation vibration modes, respectively. 1468 cm^{-1} is ascribed to —CH_3 asymmetric deformation vibration mode, whereas band at 3008 cm^{-1} is due to the characteristic =CH stretching vibration of the —HC=CH— group. After ligand-exchange process, as shown in Fig. 3(a)-B, the characteristic absorption bands of OM molecules (1084, 1581, 1468 and 3008 cm^{-1}) become inconspicuous. Simultaneously, two new bands appear locating at 1555 and 1446 cm^{-1}, corresponding to the anti-symmetric and symmetric vibration modes of the —COO^- group, respectively, indicating the adsorption of HDA on the UCNPs surface through the bidentate bonds [34]. Moreover, the stretching mode of the —COOH group at 1735 cm^{-1} suggests the presence of the free —COOH groups on the particle surface [35]. The above results indicate that the HDA molecules have replaced the original ligands on the surface of UCNPs.

Furthermore, TGA measurements were conducted to evaluate the ligand content on the NCs surface before and after the ligand exchange. TGA curves show different weight losses. In Fig. 3(b)-A, the major weight loss of 13.99% is found from 330 to 590 °C which could be due to the decomposition of OM. After ligand exchange (Fig. 3(b)-B), the major weight loss of 5.47% from 200 to 510 °C can be rationalized to the decomposition of HDA molecules. The decrease of the weight loss and the change of the decomposition temperature range also attest that OM has been replaced by HDA molecules after the ligand-exchange process (molecular weight, OM: 267.50 and HDA: 146.14). Of course, the possibility of HDA molecule chelated on UCNPs surface during the ligand-exchange process cannot be excluded (reference Scheme 1-II). In order to reduce this possibility, a large amount of ligands were added in the experiments in the reaction system (3.4 mmol), maintaining

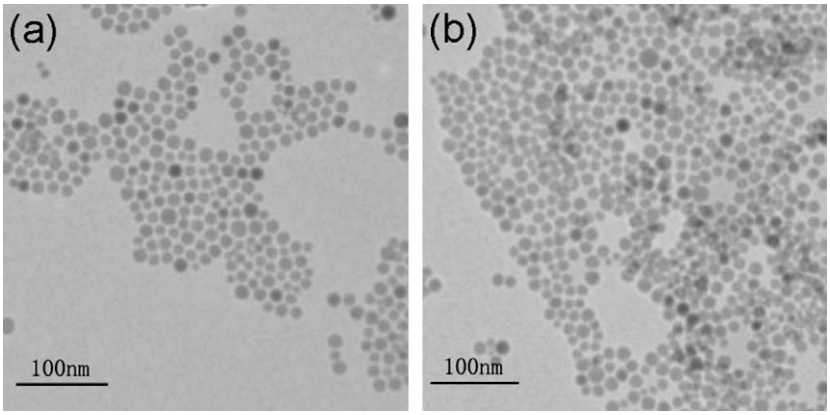

Fig. 1. TEM images of NaYF4:Yb/Er UCNPs before (a) and after (b) ligand exchange.

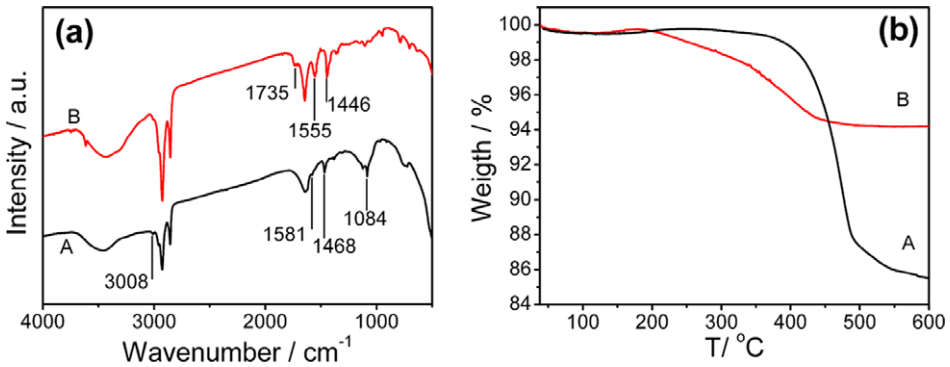

Fig. 3. (a) FT-IR spectra of the $NaYF_4$:Yb/Er UCNPs before (A) and after (B) ligand exchange using HDA. (b) TGA curves of $NaYF_4$:Yb/Er UCNPs before (A) and after (B) ligand exchange. The measurements were performed under the protection of N_2 atmosphere.

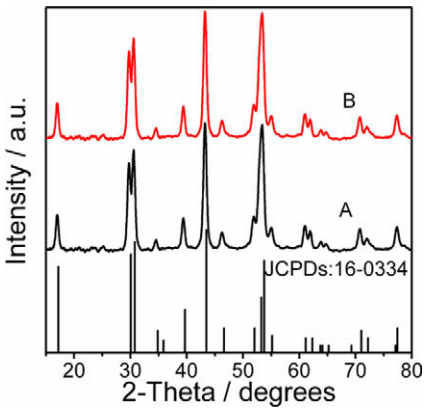

Fig. 4. XRD patterns of the original samples (A) and the HDA coated $NaYF_4$:Yb/Er UCNPs (B). The standard patterns of hexagonal (JCPDS card 16-0334) phases of $NaYF_4$ are also given.

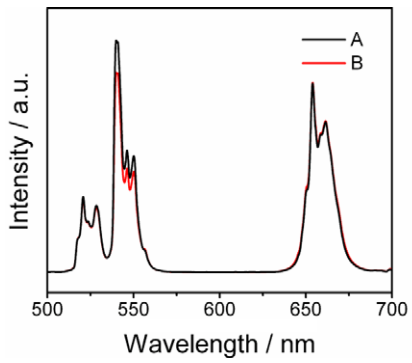

Fig. 5. Luminescence spectra of the $NaYF_4$:Yb/Er nanoparticles (0.5 mg/mL) excited with a 980-nm diode laser: (A) the original UCNPs in chloroform; (B) the HDA capped UCNPs in water.

the excessive amount of HDA molecules to competitive reaction during the exchange process.

3.3. Structure and upconversion fluorescence of the nanocrystals

XRD patterns of both the original and HDA coated $NaYF_4$:Yb/Er UCNPs were also recorded to investigate the effect of the ligand-exchange process on the structure. The XRD patterns (Fig. 4) demonstrate that the $NaYF_4$:Yb/Er UCNPs is pure hexagonal phase. The hexagonal $NaYF_4$ is yet the most efficient host material for the Yb/Er (or Yb/Tm) co-doped NIR to-visible upconversion phosphors [36]. Besides, both samples have similar phases, indicating that the high temperature ligand-exchange process has no adverse effects on the crystal structure of the UCNPs.

The upconversion luminescence properties of the UCNPs were compared before and after the ligand-exchange process. Fig. 5 shows the upconversion luminescence spectra of the original and HDA coated $NaYF_4$:20 mol% Yb, 2 mol% Er UCNPs excited with a continuous-wave 980 nm diode laser. The emission bands peaked at 521, 540, and 654 nm are attributed to $^2H_{11/2}$, $^4S_{3/2}$ and $^4F_{9/2}$ to $^4I_{15/2}$ level transitions in Er^{3+}, respectively. This ligand-exchange process has small effect on luminescence intensity. The luminescence intensity ratio ($I540/I654$) of the fluorescence spectrum is decreased from 0.79 to 0.67, which might be due to the change of surface molecules [14,15,37,38]. (Similar effect is also found for $NaYF_4$:Yb/Tm UCNPs as shown in Fig. S2 of the Supporting Information.)

3.4. Fluorescence microscopy image

In order to confirm that the hydrophilic UCNPs are suitable for biological application, the binding capacity of avidin-modified UCNPs was investigated using fluorescence microscopy image. In Fig. 6(a), the green fluorescence image is derived from UCNPs that

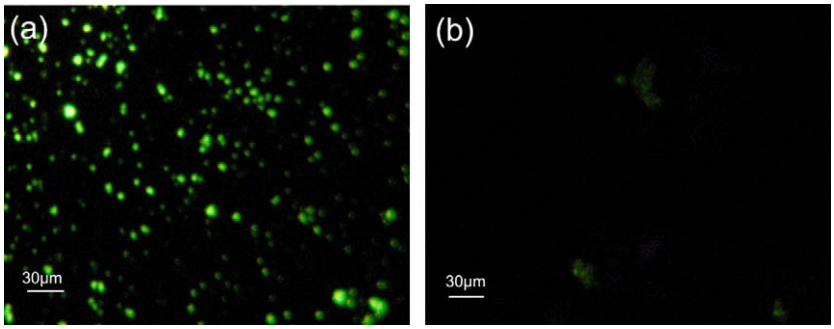

Fig. 6. Avidin-modified UCNPs as bioprobes for binding activity in vitro. The fluorescence image (a) shows avidin-coated UCNPs and biotinylated IgG bioconjugates, and (b) is the result of control experiment.

were immobilized on the surface of the plate through the interactions between avidin-coated UCNPs and biotinylated goat anti-human IgG. While in the case of the unbiotinylated antibody plate assay (Fig. 6(b)), fluorescent signal, originating from the nonspecific adsorption, is much weaker. Clearly the UCNPs, after the ligand exchange, are suitable for biological labeling.

4. Summary

In conclusion, we have developed a feasible surface–ligand-exchange method for getting water-soluble and carboxyl-functionalized UCNPs using HDA molecules at high temperature. In this exchange reaction, high concentration of the HDA molecules is kept to reduce the possibility of chelating the HDA on the particle surface. The resulting UCNPs can disperse in aqueous solution stably. TEM, DLS, XRD and PL results indicate that ligand-exchange process hardly has any adverse effects on size, crystal structure and luminescence properties of the UCNPs. Moreover, preliminary specific molecular recognition of avidin-modified UCNPs confirmed that the HDA capped UCNPs are suitable for biological labeling.

Acknowledgments

This work was supported by NSFC of China (20603035, 60601014 and 60601015), the National High Technology Development Program (2006AA03Z335), and the exchange program between CAS of China and KNAW of the Netherlands.

Appendix A. Supplementary data

TEM images of the $NaYF_4$:Yb/Tm UCNPs, luminescence spectra of the $NaYF_4$:Yb/Tm samples. Supplementary data associated with this article can be found, in the online version, at doi:10.1016/j.jcis.2009.04.024.

References

[1] L. Wang, Y. Li, Chem. Commun. (2006) 2557.
[2] D.K. Chatterjee, A.J. Rufaihah, Y. Zhang, Biomaterials 29 (2008) 937.
[3] P. Zhang, W. Steelant, M. Kumar, M. Scholfield, J. Am. Chem. Soc. 129 (2007) 4526.
[4] M. Zhang, M. Yu, F. Li, Y.M. Zhu, M. Li, Y. Gao, L. Li, Z. Liu, J. Zhang, D. Zhang, Q.T. Yi, C. Huang, J. Am. Chem. Soc. 129 (2007) 10322.
[5] W.C.W. Chan, S. Nie, Science 281 (1998) 2016.
[6] M. Bruchez Jr., M. Moronne, P. Gin, S. Weiss, A.P. Alivisatos, Science 281 (1998) 2013.
[7] I. Sondi, O. Siiman, E. Matijevi'c, J. Colloid Interface Sci. 275 (2004) 503.
[8] S.F. Lim, R. Riehn, W.S. Ryu, N. Khanarian, C. Tung, D. Tank, R.H. Austin, Nano Lett. 6 (2006) 169.
[9] G. Yi, H. Lu, S. Zhao, Y. Ge, W. Yang, D. Chen, L.H. Guo, Nano Lett. 4 (2004) 2191.
[10] K. Kuningas, T. Ukonaho, H. Päkkilä, T. Rantanen, J. Rosenberg, T. Lövgren, T. Soukka, Anal. Chem. 78 (2006) 4690.
[11] H.X. Mai, Y.W. Zhang, R. Si, Z.G. Yan, L.D. Sun, L.P. You, C.H. Yan, J. Am. Chem. Soc. 128 (2006) 6426.
[12] G.S. Yi, G.M. Chow, Adv. Funct. Mater. 16 (2006) 2324.
[13] F. Zhang, Y. Wan, T. Yu, F. Zhang, Y. Shi, S. Xie, Y. Li, L. Xu, B. Tu, D. Zhao, Angew. Chem. Int. Ed. 46 (2007) 7976.
[14] Y. Sun, Y. Chen, L. Tian, Y. Yu, X. Kong, J. Zhao, H. Zhang, Nanotechnology 18 (2007) 275609.
[15] J. Zhao, Y. Sun, X. Kong, L. Tian, Y. Wang, L. Tu, J. Zhao, H. Zhang, J. Phys. Chem. B 112 (2008) 15666.
[16] B. Dubertret, P. Skourides, D.J. Norris, V. Noireaux, A.H. Brivanlou, A. Libchaber, Science 298 (2002) 1759.
[17] Y. Wang, J.F. Wong, X. Teng, X.Z. Lin, H. Yang, Nano Lett. 3 (2003) 1555.
[18] J. Shan, Y. Ju, Appl. Phys. Lett. 91 (2007) 123103.
[19] T. Zhang, J. Ge, Y. Hu, Y. Yin, Nano Lett. 7 (2007) 3203.
[20] Z. Chen, H. Chen, H. Hu, M. Yu, F. Li, Q. Zhang, Z. Zhou, T. Yi, C. Huang, J. Am. Chem. Soc. 130 (2008) 3023.
[21] T. Pellegrino, L. Manna, S. Kudera, T. Liedl, D. Koktysh, A.L. Rogach, S. Keller, J. Rädler, G. Natile, W.J. Parak, Nano Lett. 4 (2004) 703.
[22] W.W. Yu, E. Chang, J.C. Falkner, J. Zhang, A.M.A. Somali, C.M. Sayes, J. Johns, R. Drezek, V.L. Colvin, J. Am. Chem. Soc. 129 (2007) 2871.
[23] L. Wang, Y. Li, Chem. Mater. 19 (2007) 727.
[24] Z. Zhelev, H. Ohba, R. Bakalova, J. Am. Chem. Soc. 128 (2006) 6324.
[25] S.T. Selvan, T.T. Tan, J.Y. Ying, Adv. Mater. 17 (2005) 1620.
[26] P. Yang, M. Ando, N. Murase, J. Colloid Interface Sci. 316 (2007) 420.
[27] C. Fang, B.M. Zhao, H.T. Lu, L.M. Sai, Q.L. Fan, L.H. Wang, W. Huang, J. Phys. Chem. C 112 (2008) 7278.
[28] W. Liu, H.S. Choi, J.P. Zimmer, E. Tanaka, J.V. Frangioni, M. Bawendi, J. Am. Chem. Soc. 129 (2007) 14530.
[29] W.C.W. Chan, S. Nie, Science 281 (1998) 2016.
[30] H. Mattoussi, J.M. Mauro, E.R. Goldman, G.P. Anderson, V.C. Sundar, F.V. Mikulec, M.G. Bawendi, J. Am. Chem. Soc. 122 (2000) 12142.
[31] D. Caruntu, G. Caruntu, Y. Chen, C.J. O'Connor, G. Goloverda, V.L. Kolesnichenko, Chem. Mater. 16 (2004) 5527.
[32] Y. Jun, M.F. Casula, J.H. Sim, S.Y. Kim, J. Cheon, A.P. Alivisatos, J. Am. Chem. Soc. 125 (2003) 15981.
[33] X. Ji, X. Song, J. Li, Y. Bai, W. Yang, X. Peng, J. Am. Chem. Soc. 129 (2007) 13939.
[34] A.L. Willis, N.J. Turro, S. O'Brien, Chem. Mater. 17 (2005) 5970.
[35] Y. Hu, J. Ge, Y. Sun, T. Zhang, Y. Yin, Nano Lett. 7 (2007) 1832.
[36] K.W. Krämer, D. Biner, G. Frei, H.U. Güdel, M.P. Hehlen, S.R. Lüthi, Chem. Mater. 16 (2004) 1244.
[37] F. Zhang, Y. Wan, Y. Shi, B. Tu, D. Zhao, Chem. Mater. 20 (2008) 3778.
[38] X. Bai, H. Song, G. Pan, Y. Lei, T. Wang, X. Ren, S. Lu, B. Dong, Q. Dai, L. Fan, J. Phys. Chem. C 111 (2007) 13611.